

# IDENTIFYING THE MAJOR CONTRIBUTING FACTORS FOR FOWT MOORING LINE TENSION USING ARTIFICIAL NEURAL NETWORK

Zi Lin<sup>1</sup>, Xiaolei Liu<sup>2\*</sup>

1 Department of Naval Architecture, Ocean and Marine Engineering, University of Strathclyde, Glasgow, G4 0LZ, United Kingdom

2 School of Engineering, University of Glasgow, Glasgow, G12 8QQ, United Kingdom

## ABSTRACT

Mooring lines are significant components for floating offshore wind turbines (FOWTs). Unlike offshore floating platforms, whose mooring systems are just for station-keeping, mooring lines for FOWTs are not only for station-keeping but may also have an effect on the global performance of FOWT and vice versa. Previous studies have reported mooring line damages under different operating conditions and questions have been raised about the reasons for those failures. To tackle this issue, this paper aims at studying the major contributing factors on FOWT mooring line tension. Potential influences on the mooring line fairlead tension have been grouped into forces and displacements. Using these forces and displacements as the input in an Artificial neural network (ANN) and the most loaded mooring line fairlead tension as the output, ANN was trained to investigate the significance of inputs to the mooring line tension. Under the operating condition, results from ANN showed that mooring line fairlead tension is heave motion dominated while blade root bending moment contributed first on mooring line tension in terms of forces.

**Keywords:** Floating offshore wind turbines (FOWT); Artificial neural network (ANN); Mooring line tension; Mooring damage; Dynamic response.

## 1. INTRODUCTION

As ocean renewable industry moves to deeper water depth, fixed structures gradually lose its advantages while floating platforms should be applied for deep-water structures. Learnt from offshore oil & gas

platforms, offshore floating wind turbines often apply mooring systems to prevent the platform from drifting away. Conventional mooring system can be categorized into single-point mooring and multi-point mooring, based on different types of floating structures. However, floating structures of FOWTs have seen an increasing number of diversities. Mooring systems configurations for FOWTs are almost spread moorings. Due to the water depth (less than 300m), traditional mooring chains are still popular. The influence of FOWT dynamics may have a great effect on mooring systems.

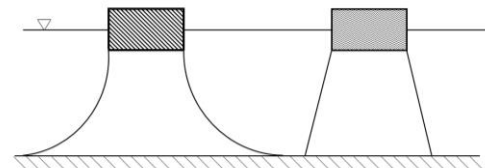


Figure 1 slack and taut mooring systems

In terms of the mooring line pattern, it can be categorized into slack and taut mooring systems. Figure 1 shows a schematic of the two types of moorings. Slack moorings often apply traditional mooring chain as mooring material. It will lose its advantage when water depth goes deeper due to the excessive weight of mooring chains and high cost. Taut moorings using more light-weight materials are suitable for deep-water applications. Currently, the water depth for FOWTs is usually less than 300 m. Therefore, slack moorings are the most conventional mooring types for FOWTs.

Previous studies have reported various mooring line failures due to different scenarios[1]. Moreover, Li, et al.[2] investigated dynamic responses of a submerged

floating wind turbine, pointing out that mooring line broken will incur an increase of platform motion. Generally speaking, there are seven mechanics contributing to mooring line failure[3]. They are wear, fatigue damage, abrasion, corrosion, damage, flawed materials, and excessive tension, respectively. Many of these failures are caused in long-term or short-term operation conditions. Among those failures, one question that needs to be asked, however, is that the major contributing factors to the failures. To tackle this problem, focusing on the mooring line failure due to excessive tension, this paper will focus on the last failure and rank the potential contributing factors for the mooring line tension.

## 2. FOWT DYNAMIC MODELLING

Compared with computational fluids dynamics methods, the Blade Element Momentum (BEM) theory, significantly saved simulation time, has been applied to evaluate wind turbine aerodynamics in this paper. The wake effect on the disturbed velocity field is improved by a correction factor. Similarly, to overcome the limitation of BEM theory, improvements on tip loss and hub loss has been developed. Further detail on the BEM theory and implementation can be found in[4].

Assuming water waves are non-rotational, inviscid and incompressible, wave forces on the FOWT platform is determined by the Laplace equation and boundary conditions. Numerical solution of the above-mentioned equations is solved via the boundary element method in the frequency domain for different wave periods. Using perturbation theory, wave forces on the platform were considered up to second order. Based on the Bernoulli's equation, wave diffraction and radiation forces are calculated in the frequency domain by WAMIT[5]. Results from frequency domain analysis were transferred to the time domain using the impulse response theory[6].

For random waves, superposition theory is applied, for which the irregular wave elevation is represented by a linear summation of different sinusoid waves[7]:

$$\xi(t) = \frac{1}{2\pi} \int_{-\infty}^{\infty} w(\omega) \sqrt{2\pi S_{\xi}(\omega)} e^{j\omega t} d\omega \quad (1)$$

where  $\xi$  denotes the wave elevation time history;  $\omega$  is the circular frequency;  $j$  is the member index;  $w(\omega)$  represents Fourier transform;  $t$  is the time and  $S_{\xi}(\omega)$  is a certain wave spectral density.

Rigid body motion equation is applied to calculate the platform 6-DOF motion responses:

$$M\ddot{X} + C\dot{X} + KX = F_1(t) + F_2(t) + F_w(t) \quad (2)$$

Where  $M$  is the mass matrix, including added mass;  $C$  the damping matrix;  $K$  the hydrostatic stiffness matrix;  $F_1$  and  $F_2$  are the first-order and second-order wave forces, respectively and  $F_w$  is the wind induced forces.

Mooring line dynamics are calculated by the lumped mass and spring model, which is one of the most widely applied numerical methods in offshore engineering. Each mooring line is divided into a series of lumped mass and connected with a spring-damper model, as shown in Figure 2. Each node's space position is determined by a vector  $r$  [8]:

$$r = \begin{Bmatrix} x_i \\ y_i \\ z_i \end{Bmatrix} \quad (3)$$

Where  $x$ ,  $y$ , and  $z$  are space coordinates and  $i$  denotes the  $i^{\text{th}}$  node.

For each segment, mooring line weight is lumped at the nodes nearby[8]:

$$W_i = \frac{1}{2}(W_{i+\frac{1}{2}} + W_{i-\frac{1}{2}})n_z \quad (4)$$

Where  $W_i$  is the net buoyancy of each segment and  $n_z$  is a unit vector in the positive  $z$  direction.

Hydrodynamic loads on the mooring line are calculated by Morison's equation. At each simulation time step, the mooring line receives position and velocity from the platform. Mooring line dynamics is then solved by the lumped-mass method, making it loosely coupled between different modules[9].

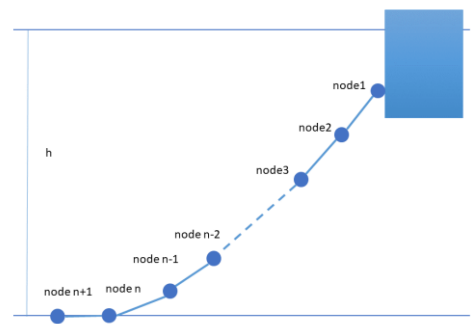


Figure2 Lumped-mass and spring model

## 3. ARTIFICIAL NEURAL NETWORK

### 3.1 Modelling Methodology

Potential influences on the mooring line fairlead tension have been grouped into forces and

displacements. Using these forces and displacements as the input for the ANN and the most loaded mooring line fairlead tension as an output, ANN was trained to study the importance of inputs on the output – most loaded mooring line fairlead tension. TensorFlow [10], which is an end-to-end open source platform for machine learning, was used here to perform a fully connected neural network model. The model itself has three layers and has been trained for 1000 epochs. Figure 3 shows a schematic of the designed ANN.

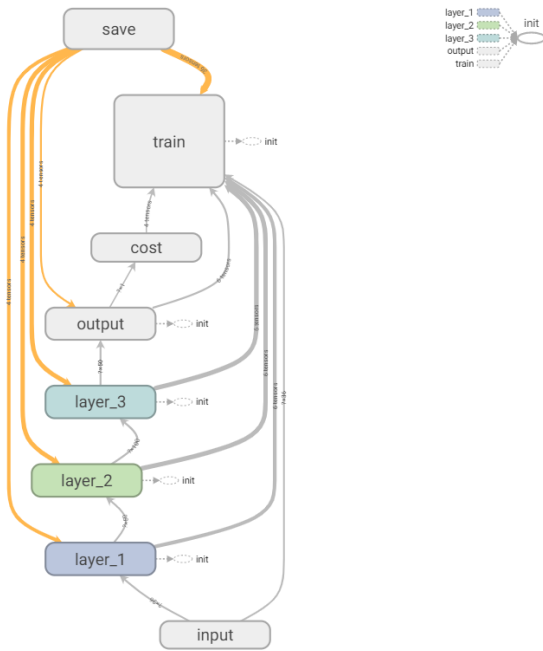


Figure 3 ANN configuration

#### 4. CASE STUDY

##### 4.1 Wind turbine properties

In the following session, a case study using the OC4 DeepWind semisubmersible is presented. Details of the structural properties of the wind turbine and the platform can be found in[11]. The FOWT is designed to operate in a water depth of 200m. There are three mooring lines in total and the angle between each adjacent mooring line is  $120^\circ$  when looking from above. Each mooring line has an unstretched length of 835.5m, making a final mooring radius of 836.6m. Further detail of the mooring properties is shown in[11].

##### 4.2 Load case definition

Focusing on operating conditions, as shown in [12], Load case 3.3 is selected as an example[12]. Wind and wave directions were co-linear and shown in Figure 4. The mean wind speed at hub height was 18m/s while the

random wave had a significant wave height of 6m and peak period of 10s. Case studies in this paper were carried out using FAST V8[13]. Turbulent wind profile was simulated in TurbSim[14]. The wind and wave spectra for simulating the sea state are Kaimal and JONSWAP, respectively. Figures 5 and 6 show time histories of horizontal wind speed and incident wave elevation at the centre of the platform, respectively.

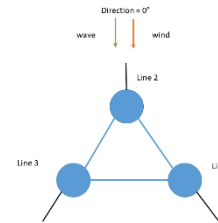


Figure 4 wind and wave directions

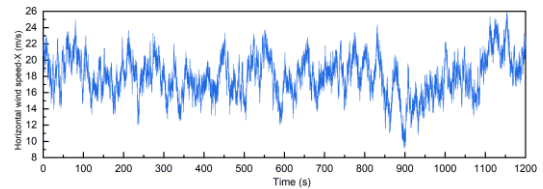


Figure 5 wind speed (horizontal-X)

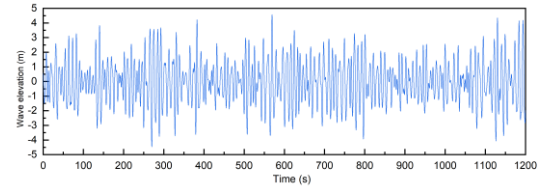


Figure 6 wave elevation

##### 4.3 Case study results and ANN ranking

Figure 7 shows the time history of the most loaded mooring line fairlead tension (line 2). Maximum mooring line tension is higher than 1800 kN and the average line tension is around 1500 kN.

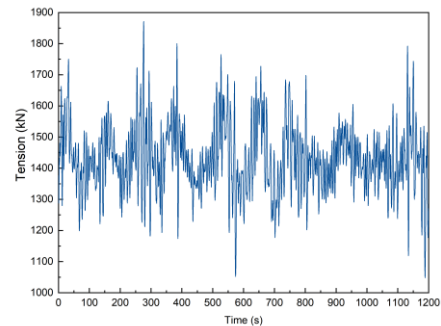


Figure 7 Fairlead tension for most loaded mooring line (line 2)

The applied ANN model is shown in session 3. The influence of displacements and forces on mooring line tension are shown in figures 8 (a) and (b). From Figure 8 (a) it can be seen that heave motion contributed most on Line 2 fairlead tension while surge motion ranked after heave. Figure 8 (a) also indicates that compared with platform motions, tower flexibility not only play an important role in wind turbine aerodynamics, especially for FOWTs but also have an effect on the mooring line tension. Figure 8(b) shows that when considering forces, blade root bending moments contribute more than turbine's tower.

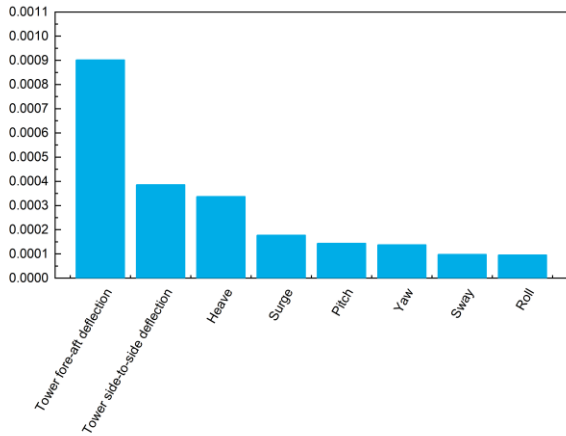


Figure 8 (a) ANN ranking, displacements

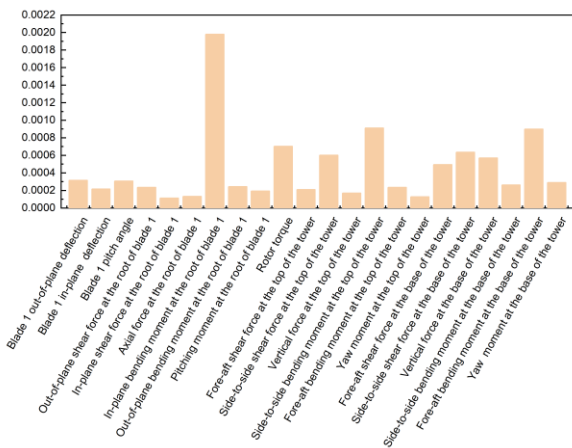


Figure 8 (b) ANN ranking, forces

## 5. CONCLUSIONS

Mooring line failures are one of the major threats for safety production of offshore wind energy sector. Previous studies have reported various mooring line failures under different conditions. However, mooring systems for FOWTs are more complicated and the

mechanism for failure is still under-investigated. This paper has presented the major contributing factors for mooring line fairlead tension, which is one of the failures during extreme conditions. For different forces, the major contributing factor is the blade root bending moment. For the 6-DOF motions, results from the trained ANN showed that mooring line fairlead tension is dominated by heave motion, which is probably due to the mooring line material (chain).

## REFERENCE

- [1] S. Gauthier and E. Elletson, "Mooring Line Monitoring to Reduce Risk of Line Failure," in *Proceedings of the Twenty-fourth (2014) International Ocean and Polar Engineering Conference*, 2014, vol. 3, pp. 388–393.
- [2] Y. Li, C. Le, H. Ding, and P. Zhang, "Dynamic Response for a Submerged Floating Off shore Wind Turbine with Different Mooring Configurations," *J. Mar. Sci. Eng.*, vol. 7, no. 115, 2019.
- [3] INTERMOOR, "Seven Mechanisms That Contribute To Mooring Line Failure." Available: <https://intermoor.com/technical-articles/six-mechanisms-that-can-contribute-to-mooring-line-failure/>.
- [4] P. J. Moriarty and A. C. Hansen, "AeroDyn Theory Manual," *NREL*, vol. 15, no. January, pp. 1–35, 2005.
- [5] WAMIT, Available: <http://www.wamit.com/>.
- [6] W. E. Cummins, "The Impulse Response Function and Ship Motions," David Taylor Model Basin, 1962.
- [7] J. M. J. Journée and W. W. Massie, *Offshore Hydromechanics*, Delft University of Technology, January, 2001.
- [8] M. Hall and A. Goupee, "Validation of a lumped-mass mooring line model with DeepCwind semisubmersible model test data," *Ocean Eng.*, vol. 104, pp. 590–603, 2015.
- [9] J. Jonkman, "The New Modularization Framework for the FAST Wind Turbine CAE Tool Preprint," *the 51<sup>st</sup> AIAA Aerospace Sciences Meeting, including the New Horizons Forum and Aerospace Exposition*, Dallas, Texas, January 7-10, 2013
- [10] "TensorFlow." Available: <https://www.tensorflow.org/>.
- [11] A. Robertson, J. Jonkman, M. Masciola, and H. Song, "Definition of the Semisubmersible Floating System for Phase II of OC4," Technical Report, NREL, 2014.
- [12] A. Robertson *et al.*, "Offshore Code Comparison Collaboration Continuation Within IEA Wind Task 30: Phase II Results Regarding a Floating Semisubmersible Wind System," *the 33<sup>rd</sup> International Conference on Ocean, Offshore and Arctic Engineering*, San Francisco, California, June 8–13, 2014
- [13] "NWTC Information Portal (FAST v8). <https://nwtc.nrel.gov/FAST8>. Last modified 04-January-2018 ; Accessed 19-May-2019."
- [14] "NWTC Information Portal (TurbSim). <https://nwtc.nrel.gov/TurbSim>. Last modified 14-June-2016 ; Accessed 18-December-2018."